Journal of Engineering Mathematics **33:** 271–291, 1998.

Exponentially accurate approximations for Dirichlet problems with discontinuous data

JAMES GEER
Department of Systems Science and Industrial Engineering, Thomas J. Watson School of Engineering and Applied Science, S.U.N.Y., Binghamton, N.Y. 13902, U.S.A.
e-mail: jgeer@binghamton.edu

Received 13 May 1997; accepted in revised form 29 December 1997

Abstract. A method to obtain exponentially accurate approximations to solutions for Dirichlet problems with discontinuous boundary data for Laplace's equation in two dimensions is presented and discussed. Model problems with circular or rectangular boundaries, whose solutions can be obtained by separation of variables involving Fourier series, are discussed in detail. First, the boundary data g is expressed as the sum of a singular function $\tilde{S}_M$, which is a certain linear combination of specially constructed 'singular basis functions' $\{S_n\}$, and a function, namely, $g - \tilde{S}_M$, which is much smoother than the original data. The function $\tilde{S}_M$ is constructed so that its discontinuities, and those of its first M derivatives, coincide with the corresponding discontinuities of g. The solution u to the boundary-value problem is then expressed as the sum of a linear combination of the harmonic extensions $\{\varphi_n\}$ of $\{S_n\}$, and a function v, which satisfies the boundary condition $v = g - \tilde{S}_M$. Since the boundary data for v has at least M continuous derivatives, the partial sum approximations for v obtained by separation of variables converge much faster than the corresponding partial sum approximations for u. Formally, by letting N, the number of terms retained in the solution for v, be proportional to M, a sequence of approximations can be constructed which converges to u exponentially in the maximum norm, as $M \to \infty$. In particular, this implies that, when g is discontinuous, the unwanted effects of the Gibbs phenomenon can be completely overcome! The method is illustrated by several examples, and some possible applications to related problems are discussed.

Key words: exponentially accurate approximation, Dirichlet, Laplace equation, Fourier series.

1. Introduction

Approximate solutions to many classes of boundary-value problems for partial differential equations are often constructed by use of a finite number of terms in a Fourier-series-type representation of the solution. In practice, this truncation procedure may lead to nonuniformly valid approximations. In particular, when a function (such as the boundary data of the problem) being approximated by its Fourier series partial sum has one or more points of simple discontinuity, Gibbs's phenomenon is present. This phenomenon typically produces several 'unwanted' effects in the partial-sum approximation, including an 'overshoot' (by about 18%) in the magnitude of the jump in the function at a point of discontinuity, as well as artificial oscillations near such a point. Unlike many other partial-sum approximations, the magnitude of the overshoot is *not eliminated* by increasing the number of terms in the approximation. In addition, the oscillations caused by this phenomenon typically propagate into regions away from the singularity, and, hence, degrade the quality of the partial-sum approximation in these regions.

In a series of papers, Gottlieb *et al.* [1–5], have proposed and investigated a way of overcoming Gibbs's phenomenon. Their technique involves the construction of a new series in-

volving Gegenbauer polynomials. For a function g that is analytic on the interval $[-1, 1]$, but is not periodic, they prove that their technique leads to a series which converges exponentially to g in the maximum norm. Recently, Geer [6] introduced and studied a class of approximations $\{F_{N,M}\}$ to a periodic function g which uses the ideas of Padé approximations based on the Fourier-series representation of g. Each approximation $F_{N,M}$ is the quotient of a trigonometric polynomial of degree N and a trigonometric polynomial of degree M. It was proven that these 'Fourier-Padé' approximations converge *point-wise* to $(g(\theta^+) + g(\theta^-))/2$ more rapidly (in some cases by a factor of $1/k^{2M}$) than the Fourier-series partial sums on which they are based. Although these approximations do *not* 'eliminate' Gibbs's phenomenon, they do mitigate its effect. In particular, the asymptotic value of the magnitude of the overshoot is reduced to about 6%, and, outside a 'small' neighborhood of a point of discontinuity of g, the 'unwanted' oscillations *can* (for practical purposes) be eliminated. Other techniques, such as those based on the Lanczos representation of a function, have also been discussed (see, *e.g.*, Lyness [7]).

More recently, Geer and Banerjee [8] (see, also, Banerjee and Geer [9]) have introduced a new, simple class of periodic 'singular basis functions', $\{S_n(\theta)\}$, which have special 'built-in' singularities. Using knowledge of the locations and magnitudes of the jumps in g and its derivatives, they prove that these functions can be used to construct a sequence of approximations which *converges exponentially* to g in the maximum norm. In particular, this implies that the Gibbs phenomenon can be completely eliminated, even when g has several points of discontinuity in the interval $[-\pi, \pi]$.

The main purpose of this paper is to apply some of the ideas presented by Geer and Banerjee [8] to a series of model boundary-value problems for Laplace's equation (Dirichlet problems), where g represents the prescribed (perhaps discontinuous) boundary data for the problem. (Although the ideas presented here will undoubtedly find applications for boundary-value problems involving more general elliptic equations, attention is restricted here to Laplace's equation, both for simplicity of presentation and for its wide range of applications.) In Section 2, the results presented in [8] are briefly summarized within the context of the current application area, and are illustrated by a simple example. In Section 3, the functions $\{S_n(\theta)\}$ are regarded as being defined on the boundary of the unit disk, and explicit, closed-form expressions for their harmonic extensions $\{\varphi_n\}$ into the interior (or exterior) of the disk are constructed. In Section 4, the functions $\{\varphi_n\}$ are used to construct a very rapidly converging sequence of approximations to the solution u to the Dirichlet problem for a disk, while, in Section 5, these ideas are extended to annular regions. In each case, it is illustrated by examples that the 'unwanted' effects of the Gibbs phenomenon are, for all practical purposes, completely eliminated. In Sections 6 and 7, Dirichlet problems for the half plane and for rectangular regions are considered, and it is again demonstrated that a new sequence of approximations can be constructed which essentially eliminates the effects of the Gibbs phenomenon. The results are discussed in Section 8.

2. Exponentially accurate approximations to discontinuous functions

To fix notation, let $g(\theta)$ be a 2π-periodic function with enough regularity so that its Fourier-series partial sums $\{G_N(\theta)\}$ converge, as $N \to \infty$, to $(g(\theta^+) + g(\theta^-))/2$, for every $\theta \in [-\pi, \pi]$, *i.e.*,

$$\lim_{N\to\infty} G_N(\theta) = \tfrac{1}{2}\left(g(\theta^+) + g(\theta^-)\right), \qquad G_N(\theta) \equiv \frac{a_0}{2} + \sum_{j=1}^{N} a_j \cos(j\theta) + b_j \sin(j\theta),$$

$$\begin{pmatrix} a_j \\ b_j \end{pmatrix} = \frac{1}{\pi}\int_{-\pi}^{\pi} g(\theta) \begin{pmatrix} \cos(j\theta) \\ \sin(j\theta) \end{pmatrix} \mathrm{d}\theta, \quad j = 0, 1, \ldots. \tag{1}$$

Here $g(\theta^+)$ $\left(g(\theta^-)\right)$ denotes the limit of g from the right (left) at θ, and both of these limits are assumed to exist and be finite. Let $C^M[-\pi, \pi]$ denote the class of 2π-periodic functions that have at least M continuous derivatives on $[-\pi, \pi]$. By repeated use of integration by parts, it is easy to show that, if $g \in C^M[-\pi, \pi]$, then the Fourier coefficients $\{a_j, b_j\}$ of g are $O(1/j^{M+2})$ as $j \to \infty$ (see, *e.g.*, Bary [10], pp. 70–80). Moreover, if g is 2π-periodic and *analytic* on $[-\pi, \pi]$, then there exists a constant ρ, with $0 < \rho < 1$, such that a_j and b_j are $O(\rho^j)$, as $j \to \infty$ (see [10], pp. 80–81). In this case, it follows that the Fourier series of g converges exponentially to g in the maximum norm.

We shall say that θ_0 is a point of *simple discontinuity* of g if

$$[g(\theta_0)] \equiv g(\theta_0^+) - g(\theta_0^-) \neq 0$$

and that θ_0 is a point of *contact discontinuity of order q* of g if

$$\left[g^{(k)}(\theta_0)\right] = 0, \quad k = 0, 1, \ldots, q-1, \quad \text{and} \quad \left[g^{(q)}(\theta_0)\right] \neq 0.$$

Here $g^{(k)}$ denotes the k^{th} derivative of g. We call a point where g has either a simple discontinuity or a contact discontinuity a point of *singularity* of the function. (We shall assume that, at each singularity, the left and right limits of each derivative of g exist and are finite.)

We now assume that g has n singularities in the interval $(-\pi, \pi]$, which lie at $\theta_1, \theta_2, \ldots, \theta_n$, and we let $\left[g^{(k)}(\theta_s)\right]$, $k = 0, 1, \ldots$, denote the jump in the kth derivative of g at $\theta = \theta_s$. In [8], a special class of 2π-periodic basis functions $\{S_n(\theta)\}$, which have certain 'built-in' singularities, were introduced and studied. In particular, it was shown how they could be used to construct a new sequence of approximations which, although based on the Fourier-series partial-sum approximations to g, converges exponentially to g in the maximum norm. In particular, this implies that this new sequence of approximations completely eliminates Gibbs's phenomenon. For completeness, we now briefly summarize how these approximations can be constructed. (See [8] for more details.)

The functions $\{S_n(\theta)\}$ are defined by

$$S_{2k}(\theta) \equiv \frac{2^{k-3/2}}{(2k)!} \sin(\theta)(1 - \cos(\theta))^{k-1/2} = \sum_{j=1}^{\infty} b_{2k,j} \sin(j\theta), \tag{2}$$

$$S_{2k+1}(\theta) \equiv \frac{2^{k-1/2}}{(2k+1)!}(1 - \cos(\theta))^{k+1/2} = \frac{a_{2k+1,0}}{2} + \sum_{j=1}^{\infty} a_{2k+1,j} \cos(j\theta), \tag{3}$$

$$a_{2k+1,j} = (-1)^{k+1}\frac{4^{k+1}}{\pi}\frac{1}{\prod_{i=0}^{k}(4j^2-(2i+1)^2)}, \qquad b_{2k,j} = -ja_{2k+1,j}, \tag{4}$$

for $j = 0, 1, 2, \ldots$, and $k = 0, 1, 2, \ldots$. It is straightforward to show that $S_n(\theta)$ is $C^{n-1}[-\pi, \pi]$, while the jump in its nth derivative at $\theta = 0$ is 1, *i.e.*,

$$[S_n^{(q)}(0)] \equiv \left[\left(\frac{\mathrm{d}}{\mathrm{d}\theta}\right)^q S_n(\theta)\right]_{\theta=0} = 0, \quad \text{if } q < n; \qquad [S_n^{(n)}(0)] = 1. \tag{5}$$

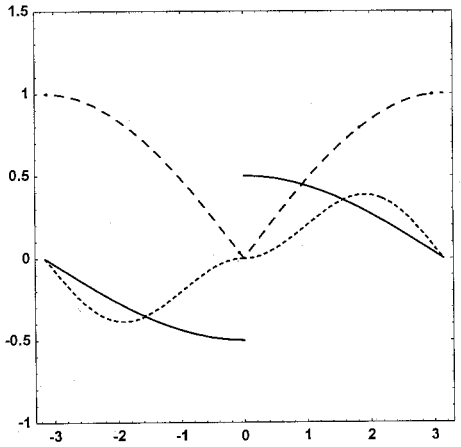

Figure 1. The singular basis functions $S_0(\theta)$ (solid line), $S_1(\theta)$ (dashed line), and $S_2(\theta)$ (dotted line), defined in Equations (2)–(3).

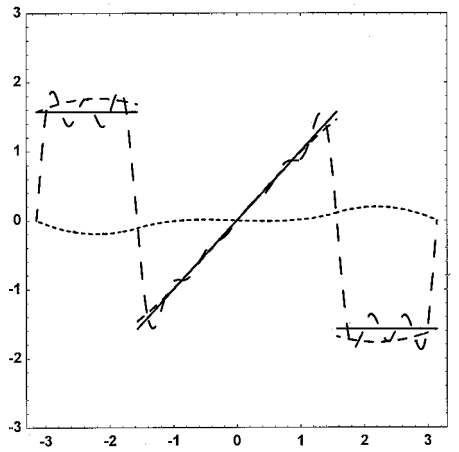

Figure 2. The function $g(\theta)$ (solid line) from (11), its Fourier series partial sum $G_{11}(\theta)$ (long dashed line) from (1) with $N = 11$, $\tilde{S}_1(\theta)$ (dashed line) from (12), and the difference $g(\theta) - \tilde{S}_1(\theta)$ (dotted line). Note that the difference $g(\theta) - \tilde{S}_1(\theta)$ is much smoother than either $g(\theta)$ or $\tilde{S}_1(\theta)$.

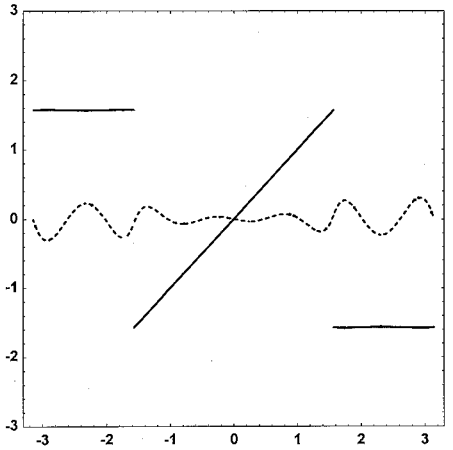

Figure 3. The approximation $g^{(1,4)}(\theta)$ (solid line) from (8), with $M = 1$ and $N = 4$, and the magnified error $50 \cdot (g(\theta) - g^{(1,4)}(\theta))$ (dotted line) for the example of Section 2.

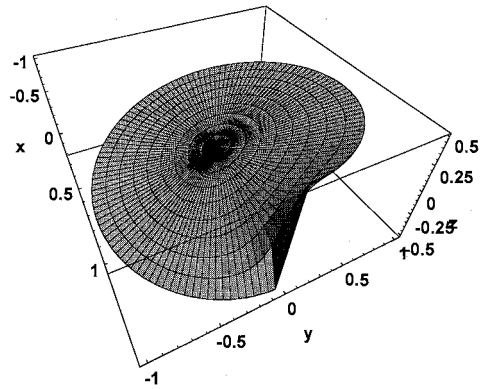

Figure 4. A surface plot of the harmonic extension $\varphi_0(r, \theta)$ (Equation (14)) of $S_0(\theta)$ into the interior of the unit circle.

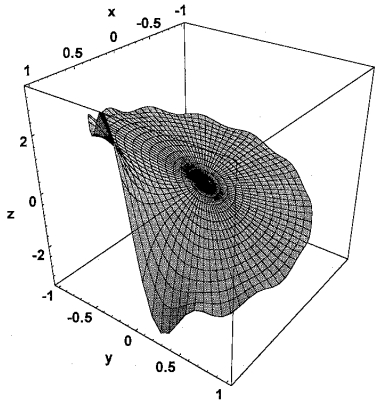

Figure 5. The approximation $u_{11}(r, \theta)$ from (18) with $N = 11$ for the example of Section 4.

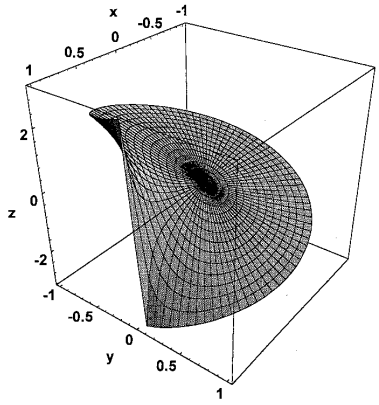

Figure 6. The approximation $u^{(0,4)}(r, \theta)$ from (21)–(22) with $M = 0$ and $N = 4$ for the example of Section 4.

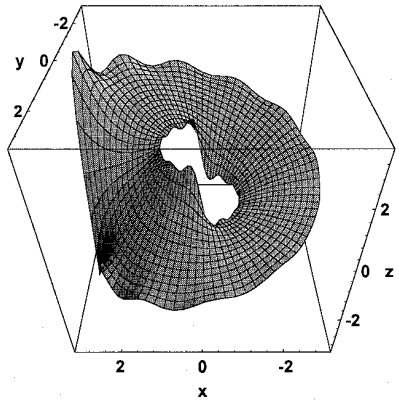

Figure 7. The approximation $u_{11}(r, \theta)$ from (25) with $N = 11$ for the example of Section 5.

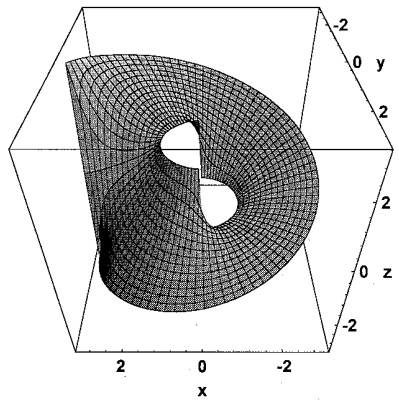

Figure 8. The approximation $u^{(0,4)}(r, \theta)$ from (32)–(33) with $M = 0$ and $N = 4$ for the example of Section 5.

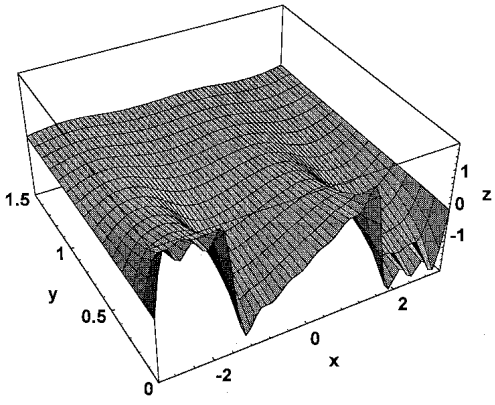

Figure 9. The approximation $u_{11}(x, y)$ from (41) with $N = 11$ for the example of Section 6.

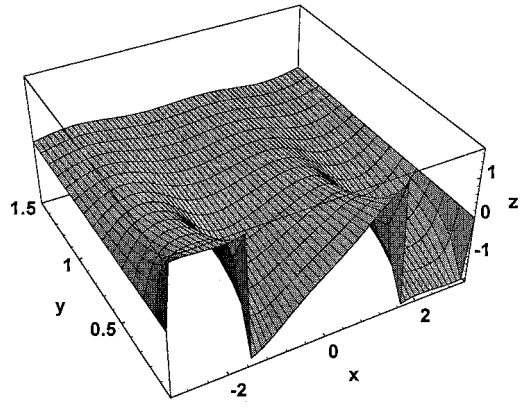

Figure 10. The approximation $u^{(0,3)}(x, y)$ from (47)–(48) with $M = 0$ and $N = 3$ for the example of Section 6.

The functions S_0, S_1, and S_2 are plotted in Figure 1.

To construct a new sequence of approximations to g, we first define

$$\tilde{S}_M(\theta) \equiv \sum_{k=0}^{M} \sum_{s=1}^{n} A_{k,s} S_k(\theta - \theta_s), \tag{6}$$

where the constants $\{A_{k,s}\}$ are determined so that the jumps in $\tilde{S}_M$, and its first M derivatives, coincide with the corresponding jumps in g, *i.e.*, so that $g(\theta) - \tilde{S}_M(\theta)$ is $C^M[-\pi, \pi]$. Using the properties (5), we find that these constants can be determined recursively from the relations

$$A_{k,s} = \left[g^{(k)}(\theta_s)\right] - \sum_{i=0}^{k-1} A_{i,s} \left[S_i^{(k)}(0)\right], \quad s = 1, 2, \ldots n, \quad k = 0, 1, \ldots, M. \tag{7}$$

Thus, the function $g(\theta) - \tilde{S}_M(\theta)$ is $C^M[-\pi, \pi]$, at least, and hence its Fourier series converges at a faster rate than the Fourier series of g. Once $\tilde{S}_M(\theta)$ has been defined, we define the family of approximations $\left\{g^{(M,N)}\right\}$ to g by

$$g^{(M,N)}(\theta) \equiv \tilde{S}_M(\theta) + \frac{\tilde{a}_0^{(M)}}{2} + \sum_{j=1}^{N} \tilde{a}_j^{(M)} \cos(j\theta) + \tilde{b}_j^{(M)} \sin(j\theta), \tag{8}$$

$$\tilde{a}_j^{(M)} = a_j - \sum_{k=0}^{M} \sum_{s=1}^{n} A_{k,s} \left\{a_{k,j} \cos(j\theta_s) - b_{k,j} \sin(j\theta_s)\right\}, \tag{9}$$

$$\tilde{b}_j^{(M)} = b_j - \sum_{k=0}^{M} \sum_{s=1}^{n} A_{k,s} \left\{a_{k,j} \sin(j\theta_s) + b_{k,j} \cos(j\theta_s)\right\}, \quad j = 0, 1, 2, \ldots, N, \tag{10}$$

where it is understood that $a_{n,j} = 0$, if n is even, and $b_{n,j} = 0$, if n is odd. Here we note that the partial sum in (8) is just the Fourier-series partial-sum approximation to the difference $g - \tilde{S}_M$.

The approximations $\{g^{(M,N)}\}$ have several useful convergence properties. In particular, if we let N be proportional to M, say, $N = \lambda M$, for a suitable constant λ, *then the sequence* $\{g^{(M,\lambda M)}\}$ *converges exponentially to* g *in the maximum norm for all* $-\pi \leqslant \theta \leqslant \pi$, *as* $M \to \infty$. *As a consequence, this implies that Gibbs's phenomenon, and its effects, can be completely eliminated* (see [8]). In addition, *each derivative of* $\{g^{(M,\lambda M)}\}$ *converges exponentially, as* $M \to \infty$, *to the corresponding derivative of* g *in the maximum norm for all* $-\pi \leqslant \theta \leqslant \pi$.

To illustrate these approximations, we let

$$g(x) = \begin{cases} \frac{1}{2}\pi, & -\pi < x < -\frac{1}{2}\pi, \\ x, & -\frac{1}{2}\pi < x < \frac{1}{2}\pi, \\ -\frac{1}{2}\pi, & \frac{1}{2}\pi < x < \pi, \end{cases} \tag{11}$$

from which we find $a_j = 0$, $j \geqslant 0$, and $b_j = (-1)^j/j - (2/j)\cos(j\pi/2) + (2/\pi j^2)\sin(j\pi/2)$, $j \geqslant 1$. The function $g(\theta)$ and its Fourier-series partial sum $G_{11}(\theta)$, from (1) with $N = 11$, are plotted in Figure 2.

To construct a 'better' approximation to g, we first note that g has three singularities in the interval $(-\pi, \pi]$, and hence we set $n = 3$, with $\theta_1 = -\pi/2$, $\theta_2 = \pi/2$, and $\theta_3 = \pi$. From the definition of g and (7), we find $A_{0,1} = -\pi$, $A_{0,2} = -\pi$, $A_{0,3} = \pi$, $A_{1,1} = 1$, $A_{1,2} = -1$, and $A_{1,3} = 0$. Then, using these values in (6), we define

$$\tilde{S}_1(\theta) \equiv -\pi S_0(\theta + \tfrac{1}{2}\pi) - \pi S_0(\theta - \tfrac{1}{2}\pi) + \pi S_0(\theta - \pi) + S_1(\theta + \tfrac{1}{2}\pi) - S_1(\theta - \tfrac{1}{2}\pi). \quad (12)$$

The function $\tilde{S}_1(\theta)$ and the difference $g(\theta) - \tilde{S}_1(\theta)$ are also plotted in Figure 2. Note that, by the way $\tilde{S}_1(\theta)$ has been defined, the difference $g(\theta) - \tilde{S}_1(\theta)$ is $C^1[-\pi, \pi]$ and, hence, is much smoother than the original function $g(\theta)$. The Fourier coefficients $\{\tilde{a}_j^{(1)}\}$ and $\{\tilde{b}_j^{(1)}\}$ of $g(\theta) - \tilde{S}_1(\theta)$, defined in Equations (9)–(10), are given by

$$\tilde{a}_j^{(1)} = 0, \quad j \geqslant 0, \qquad \tilde{b}_j^{(1)} = \frac{j\pi(2\cos(j\pi/2) - (-1)^j) - 2\sin(j\pi/2)}{\pi j^2(4j^2 - 1)}, \quad j \geqslant 1.$$

(Note that the coefficients $\tilde{b}_j^{(1)}$ are $O(1/j^3)$, as $j \to \infty$, whereas the original coefficients b_j are only $O(1/j)$, as $j \to \infty$). In Figure 3, the approximation $g^{(1,4)}(\theta)$ (Equation (8), with $M = 1$ and $N = 4$) and the magnified error $50 \times (g(\theta) - g^{(1,4)}(\theta))$ are plotted. The figure clearly illustrates the quality of the approximation $g^{(1,4)}$, especially when compared with the Fourier-series partial sum G_{11} (see Figure 2), even though the latter contains several more terms.

We now apply some of these ideas to a variety of two-dimensional boundary-value-problems involving Laplace's equation. We begin with problems which can be conveniently expressed in terms of polar coordinates, and then consider problems expressed in terms of rectangular coordinates.

3. Harmonic extensions of the singular basis functions $S_n(\theta)$ into circular domains

We first wish to consider some classes of boundary-value problems for which $g(\theta)$ represents the boundary data of the problem, defined on the unit circle $r = 1$. Since we will be using the functions $\{S_n(\theta)\}$ to help construct 'better' approximations to $g(\theta)$, and, ultimately, to construct 'better' approximations to the solution to a boundary-value problem, in this section we construct the harmonic extension $\varphi_n(r, \theta)$ of S_n into the interior (or exterior) of the unit circle. Thus, for the interior problem, φ_n is the solution of the boundary-value problem

$$\nabla^2\varphi_n(r, \theta) = 0, \quad 0 \leqslant r < 1, \quad 0 \leqslant \theta \leqslant 2\pi, \quad \text{with } \varphi_n(1, \theta) = S_n(\theta).$$

To construct φ_n, we first use (2)–(4) to write

$$S_n(\theta) = \frac{a_{n,0}}{2} + \sum_{j=1}^{\infty} a_{n,j}\cos(j\theta) + b_{n,j}\sin(j\theta), \quad n = 0, 1, 2, \ldots,$$

and then, for any value of r, with $0 \leqslant r \leqslant 1$, we define

$$\varphi_n(r, \theta) = \frac{a_{n,0}}{2} + \sum_{j=1}^{\infty} r^j\{a_{n,j}\cos(j\theta) + b_{n,j}\sin(j\theta)\}$$

$$= \operatorname{Re}\left\{\frac{a_{n,0}}{2} + \sum_{j=1}^{\infty}(a_{n,j} + ib_{n,j})w^j\right\}, \quad w = r\,\mathrm{e}^{-i\theta}. \quad (13)$$

Since $S_n(\theta)$ is piece-wise smooth, the series in (13) converges sufficiently well so that $\nabla^2\varphi_n = 0$, for $0 \leqslant r < 1$, and $\varphi_n = S_n(\theta)$ on $r = 1$. (The analogous expression for the extension of S_n into the exterior of the unit circle, which is bounded as $r \to \infty$, is given by (13) with r replaced by $1/r$.)

Because of the relative simplicity of the coefficients $\{a_{n,j}, b_{n,j}\}$, it is possible to sum the series in (13) for any nonnegative integer n, and, hence, to determine an explicit, closed-form solution for each $\varphi_n(r, \theta)$. In particular, using (2)–(4), and (13), we find (using *Mathematica* [11], p. 104)

$$\begin{aligned}\varphi_0(r,\theta) &= -\frac{1}{\pi}\,\mathrm{Im}\left\{\frac{1+w}{\sqrt{w}}\,\tanh^{-1}\sqrt{w}\right\}\\ &= \frac{1}{2\pi}\left\{\frac{1+r}{\sqrt{r}}\,\cos(\theta/2)\cdot AT - \frac{1-r}{2\sqrt{r}}\,\sin(\theta/2)\cdot L\right\},\end{aligned} \tag{14}$$

$$\begin{aligned}\varphi_1(r,\theta) &= \frac{2}{\pi}\,\mathrm{Re}\left\{\frac{1-w}{\sqrt{w}}\,\tanh^{-1}\sqrt{w}\right\}\\ &= \frac{1}{2\pi}\left\{\frac{1-r}{\sqrt{r}}\,\cos(\theta/2)\cdot L + 2\frac{1+r}{\sqrt{r}}\,\sin(\theta/2)\cdot AT\right\},\end{aligned} \tag{15}$$

where

$$AT \equiv \tan^{-1}\left(\frac{2\sqrt{r}\,\sin(\theta/2)}{1-r}\right), \qquad L \equiv \log\left(\frac{1+r+2\sqrt{r}\,\cos(\theta/2)}{1+r-2\sqrt{r}\cos(\theta/2)}\right).$$

Analogous expressions hold for φ_n, with $n \geqslant 2$. The function φ_0 is plotted in Figure 4.

We shall now use the functions $\{\varphi_n\}$ to construct approximations to two classes of problems involving Laplace's equations in regions with circular boundaries, which converge to the exact solution of the problem much faster than the Fourier-series-type solutions on which they are based.

4. Dirichlet problem in a disk

We consider first the simple Dirichlet problem for $u\,(r, \theta)$ given by

$$\nabla^2 u = 0, \quad 0 \leqslant r < 1, \quad 0 \leqslant \theta \leqslant 2\pi, \tag{16}$$

$$u = g(\theta), \quad \text{on } r = 1. \tag{17}$$

Here the prescribed boundary data g is assumed to have n singularities in the interval $(-\pi, \pi]$, which lie at $\theta_1, \theta_2, \ldots, \theta_n$. A straightforward use of separation of variables leads to the family of approximate solutions

$$u_N(r,\theta) = \frac{a_0}{2} + \sum_{j=1}^{N} r^j\left(a_j\,\cos(j\theta) + b_j\,\sin(j\theta)\right), \quad N = 1, 2, \ldots, \tag{18}$$

where $\{a_j, b_j\}$ are the Fourier coefficients of g defined in (1).

To construct a more rapidly converging sequence of approximations to u, for any non-negative integer M we first define $\tilde{S}_M(\theta)$, given by (6), in terms of the singularities of g, as in Section 2, and then define

$$\tilde{\varphi}_M(r,\theta) \equiv \sum_{k=0}^{M} \sum_{s=1}^{n} A_{k,s}\varphi_k(r,\theta-\theta_s). \tag{19}$$

Here the constants $\{A_{k,s}\}$ are defined in (7) in terms of the singularities of g, and the harmonic functions $\{\varphi_k\}$ are defined in Section 3. In particular, we note that the locations and magnitudes of the singularities of $\tilde{\varphi}_M(1,\theta) = \tilde{S}_M(\theta)$, up to and including the Mth derivative, coincide with those of $g(\theta)$.

We now look for a solution for u in the form

$$u(r,\theta) = \tilde{\varphi}_M(r,\theta) + v(r,\theta), \tag{20}$$

where v must be determined. Using Equations (19)–(20) in Equations (16)–(17), we find that v satisfies

$$\nabla^2 v = 0, \quad 0 \leqslant r < 1, \quad 0 \leqslant \theta \leqslant 2\pi,$$

with

$$v = g(\theta) - \tilde{S}_M(\theta), \quad \text{on } r = 1.$$

We note that the boundary data for v is at least $C^M[-\pi,\pi]$ and, hence, the Fourier-series-type solution for v, analogous to (18), will converge faster than the corresponding approximate solutions $\{u_N\}$ (Equation (18)) for u. Thus, we solve the problem for v by separation of variables and then, for any positive integer N, we define new approximations $u^{(M,N)}$ for u as

$$u^{(M,N)}(r,\theta) = \tilde{\varphi}_M(r,\theta) + v^{(M,N)}(r,\theta), \tag{21}$$

with

$$v^{(M,N)}(r,\theta) = \frac{\tilde{a}_0^{(M)}}{2} + \sum_{j=1}^{N} r^j(\tilde{a}_j^{(M)}\cos(j\theta) + \tilde{b}_j^{(M)}\sin(j\theta)), \tag{22}$$

where the coefficients $\{\tilde{a}_j^{(M)}, \tilde{b}_j^{(M)}\}$, which are defined in (9)–(10), are just the Fourier coefficients of $g(\theta) - \tilde{S}_M(\theta)$. (The corresponding approximations which are valid in the region exterior to the unit disk, and which remain bounded as $r \to \infty$, are given by (21)–(22), with r replaced by $1/r$.)

To illustrate these results, we let $g(\theta) = \theta - \pi$, for $0 < \theta < 2\pi$, from which we find $a_j = 0$, $j \geqslant 0$, and $b_j = -2/j$, $j \geqslant 1$. In Figure 5 we have plotted u_{11} obtained by using these coefficients in (18) with $N = 11$. To construct a better approximation to u, we use the definition of g to set $n = 1$, with $\theta_1 = 0$ and $[g(\theta_1)] = -2\pi$. We then set $M = 0$ in (19) and, using $A_{0,1} = -2\pi$, from (7), we find

$$\tilde{\varphi}_0(r,\theta) = -2\pi\varphi_0(r,\theta).$$

Then, using (9)–(10), we find

$$\tilde{a}_j^{(0)} = 0, \quad j \geqslant 0, \qquad \tilde{b}_j^{(0)} = \frac{2}{j(4j^2-1)}, \quad j \geqslant 1.$$

(Note that $\tilde{b}_j^{(0)} = O(1/j^3)$, as $j \to \infty$, whereas the original Fourier coefficients $b_j = O(1/j)$, as $j \to \infty$.) In Figure 6 we have plotted $u^{(0,4)}$ obtained by using these results in Equations (21)–(22) with $M = 0$ and $N = 4$. Figures 5 and 6 illustrate the improved quality of the approximation $u^{(0,4)}$, compared to u_{11}. In fact, the L_∞ norm of the difference $u - u_{11}$ is

$$\|u - u_{11}\|_\infty \equiv \max_{\substack{0 \leqslant r \leqslant 1 \\ 0 \leqslant \theta \leqslant 2\pi}} |u(r,\theta) - u_{11}(r,\theta)| = \max_{0 \leqslant \theta \leqslant 2\pi} |u(1,\theta) - u_{11}(1,\theta)| \cong 3{\cdot}14,$$

while

$$\|u - u^{(0,4)}\|_\infty \cong 9{\cdot}46 \times 10^{-3}.$$

5. Dirichlet problem in an annular region

We next consider the Dirichlet problem for $u(r,\theta)$ in an annular region, defined by

$$\nabla^2 u = 0, \quad 0 < r_i < r < r_o, \quad 0 \leqslant \theta \leqslant 2\pi, \tag{23}$$

$$u = g_i(\theta), \quad \text{for } r = r_i, \quad \text{and} \quad u = g_o(\theta), \quad \text{for } r = r_o. \tag{24}$$

Here the constants $r_i > 0$ and $r_o > r_i$ are specified, and the prescribed boundary data g_i and g_o are assumed to have singularities in the interval $(-\pi, \pi]$, which lie at $\theta = \theta_{i,1}$, $\theta_{i,2}, \ldots, \theta_{i,n_i}$ and $\theta = \theta_{o,1}, \theta_{o,2}, \ldots, \theta_{o,n_o}$, respectively. Separation of variables leads to the family of approximate solutions

$$\begin{aligned} u_N(r,\theta) \equiv\ & \frac{a_0^i}{2} + \frac{a_0^o - a_0^i}{2} \frac{\log(r/r_i)}{\log(r_o/r_i)} \\ & + \sum_{j=1}^{N} \left\{ \left(a_j^o \left(\frac{r_o}{r}\right)^j \frac{r^{2j} - r_i^{2j}}{r_o^{2j} - r_i^{2j}} + a_j^i \left(\frac{r_i}{r}\right)^j \frac{r_o^{2j} - r^{2j}}{r_o^{2j} - r_i^{2j}} \right) \cos(j\theta) \right. \\ & \left. + \left(b_j^o \left(\frac{r_o}{r}\right)^j \frac{r^{2j} - r_i^{2j}}{r_o^{2j} - r_i^{2j}} + b_j^i \left(\frac{r_i}{r}\right)^j \frac{r_o^{2j} - r^{2j}}{r_o^{2j} - r_i^{2j}} \right) \sin(j\theta) \right\}, \end{aligned} \tag{25}$$

where $\{a_j^i, b_j^i\}$ and $\{a_j^o, b_j^o\}$ are the Fourier coefficients of g^i and g^o, respectively.

To construct a 'better' approximation to u, we follow the ideas of the previous section and first define the harmonic functions

$$\tilde{\varphi}_M^i(r,\theta) \equiv \sum_{k=0}^{M} \sum_{s=1}^{n_i} A_{k,s}^i \varphi_k(r_i/r, \theta - \theta_{i,s}), \tag{26}$$

and

$$\tilde{\varphi}_M^o(r,\theta) \equiv \sum_{k=0}^{M} \sum_{s=1}^{n_o} A_{k,s}^o \varphi_k(r/r_o, \theta - \theta_{o,s}). \tag{27}$$

Here the constants $\{A_{k,s}^i\}$ and $\{A_{k,s}^o\}$ are defined by (7) in terms of the singularities of g^i and g^o, respectively, and the functions $\{\varphi_k\}$ are defined in Section 3. We then look for a solution for u in the form

$$u(r,\theta) = \tilde{\varphi}_M^i(r,\theta) + \tilde{\varphi}_M^o(r,\theta) + v(r,\theta), \tag{28}$$

where v satisfies

$$\nabla^2 v = 0, \quad 0 < r_i < r < r_o, \quad 0 \leqslant \theta \leqslant 2\pi, \tag{29}$$

with

$$v = \{g_i(\theta) - \tilde{\varphi}_M^i(r_i,\theta)\} - \tilde{\varphi}_M^o(r_i,\theta), \quad \text{on } r = r_i, \tag{30}$$

and

$$v = \{g_o(\theta) - \tilde{\varphi}_M^o(r_o,\theta)\} - \tilde{\varphi}_M^i(r_o,\theta), \quad \text{on } r = r_o. \tag{31}$$

Thus, we can determine v in a straightforward manner, using separation of variables. Here we note that, in each of the boundary conditions for v, the term in brackets on the right side of each equation is $C^M[-\pi,\pi]$, at least, while the last term is analytic for $0 \leqslant \theta \leqslant 2\pi$. Thus, the boundary conditions for v are much smoother than the corresponding conditions for u, and, hence, the solution for v obtained by separation of variables will converge much faster than the corresponding solution for u.

Once the functions $\tilde{\varphi}_M^i$ and $\tilde{\varphi}_M^o$ have been defined, for any positive integer N, we define the new approximations

$$u^{(M,N)}(r,\theta) = \tilde{\varphi}_M^i(r,\theta) + \tilde{\varphi}_M^o(r,\theta) + v^{(M,N)}(r,\theta), \tag{32}$$

where $v^{(M,N)}$ is a partial-sum approximation to v, obtained by separation of variables, and is given by

$$\begin{aligned} v^{(M,N)}(r,\theta) \;\equiv\; & \frac{\tilde{a}_0^i}{2} + \frac{\tilde{a}_0^o - \tilde{a}_0^i}{2} \frac{\log(r/r_i)}{\log(r_o/r_i)} \\ & + \sum_{j=1}^{N} \left\{ \left(\tilde{a}_j^o \left(\frac{r_o}{r}\right)^j \frac{r^{2j} - r_i^{2j}}{r_o^{2j} - r_i^{2j}} + \tilde{a}_j^i \left(\frac{r_i}{r}\right)^j \frac{r_o^{2j} - r^{2j}}{r_o^{2j} - r_i^{2j}} \right) \cos(j\theta) \right. \\ & \left. + \left(\tilde{b}_j^o \left(\frac{r_o}{r}\right)^j \frac{r^{2j} - r_i^{2j}}{r_o^{2j} - r_i^{2j}} + \tilde{b}_j^i \left(\frac{r_i}{r}\right)^j \frac{r_o^{2j} - r^{2j}}{r_o^{2j} - r_i^{2j}} \right) \sin(j\theta) \right\}. \end{aligned} \tag{33}$$

Here, the coefficients $\{\tilde{a}^i_j, \tilde{b}^i_j\}$ are defined by (see Equations (9)–(10))

$$\tilde{a}^i_j = a^i_j - \sum_{k=0}^{M}\sum_{s=1}^{n_i} A^i_{k,s}\left\{a_{k,j}\cos(j\theta_{i,s}) - b_{k,j}\sin(j\theta_{i,s})\right\}$$
$$-\left(\frac{r_i}{r_o}\right)^j \sum_{k=0}^{M}\sum_{s=1}^{n_o} A^o_{k,s}\left\{a_{k,j}\cos(j\theta_{o,s}) - b_{k,j}\sin(j\theta_{o,s})\right\},$$

$$\tilde{b}^i_j = b^i_j - \sum_{k=0}^{M}\sum_{s=1}^{n_i} A^i_{k,s}\left\{a_{k,j}\sin(j\theta_{i,s}) + b_{k,j}\cos(j\theta_{i,s})\right\}$$
$$-\left(\frac{r_i}{r_o}\right)^j \sum_{k=0}^{M}\sum_{s=1}^{n_o} A^o_{k,s}\left\{a_{k,j}\sin(j\theta_{o,s}) + b_{k,j}\cos(j\theta_{o,s})\right\}, \tag{34}$$

for $j = 0, 1, 2, \ldots, N$. The expressions for $\tilde{a}^o_j$ and $\tilde{b}^o_j$ are given by (34), with a^i_j, b^i_j, $A^i_{k,s}$, $A^o_{k,s}$, $\theta_{i,s}$, $\theta_{o,s}$, n_i, and n_o replaced by a^o_j, b^o_j, $A^o_{k,s}$, $A^i_{k,s}$, $\theta_{o,s}$, $\theta_{i,s}$, n_o, and n_i, respectively.

To illustrate these results, we let

$$g_i = \begin{cases} 1, & -\pi/2 < \theta < \pi/2, \\ -1, & \pi/2 < \theta < 3\pi/2, \end{cases}$$
$$a^i_0 = 0, \qquad a^i_j = \frac{4\,\sin(j\pi/2)}{\pi j}, \qquad b^i_j = 0, \quad j \geqslant 1, \tag{35}$$

and

$$g_o = \theta - \pi, \quad 0 < \theta < 2\pi, \qquad a^o_j = 0, \quad j \geqslant 0, \qquad b^o_j = -2/j, \quad j \geqslant 1, \tag{36}$$

with $r_i = 1$ and $r_o = 3$. In Figure 7 we have plotted u_{11} obtained by using these coefficients in (25) with $N = 11$. To construct a 'better' approximation to u, we use the definitions of g_i and g_o to find $n_i = 2$, with $\theta_{i,1} = -\pi/2$, $[g(\theta_{i,1})] = 2$, $\theta_{i,2} = \pi/2$, $[g(\theta_{i,2})] = -2$, and $n_o = 1$, with $\theta_{o,1} = 0$ and $[g(\theta_{o,1})] = -2\pi$. We then set $M = 0$ in Equations (26)–(27) and, using $A^i_{0,1} = 2 = -A^i_{0,2}$ and $A^o_{0,1} = -2\pi$, from (7), we find

$$\tilde{\varphi}^i_0(r,\theta) = 2\varphi_0(r_i/r, \theta + \pi/2) - 2\varphi_0(r_i/r, \theta - \pi/2),$$
$$\tilde{\varphi}^o_0(r,\theta) = -2\pi\varphi_0(r/r_o, \theta). \tag{37}$$

Also, from (34) we find

$$\tilde{a}^i_0 = 0, \qquad \tilde{a}^i_j = \frac{4\,\sin(j\pi/2)}{\pi j(1-4j^2)}, \qquad \tilde{b}^i_j = \frac{8j}{4j^2-1}\cdot\left(\frac{r_i}{r_o}\right)^j, \quad j \geqslant 1,$$
$$\tilde{a}^o_0 = 0, \qquad \tilde{a}^o_j = \frac{16j\,\sin(j\pi/2)}{\pi(1-4j^2)}\cdot\left(\frac{r_i}{r_o}\right)^j, \qquad \tilde{b}^o_j = \frac{2}{j(4j^2-1)}, \quad j \geqslant 1. \tag{38}$$

In Figure 8 we have plotted $u^{(0,4)}$ obtained by using (37)–(38) in (32)–(33) with $M = 0$ and $N = 4$. One reason for the obvious improvement of $u^{(0,4)}$ over u_{11} is the behavior, as $j \to \infty$, of the coefficients defined in (38). In particular, we note that, whereas the original Fourier coefficients ((35)–(36)) of g_i and g_o are $O(1/j)$, as $j \to \infty$, the coefficients $\tilde{a}_j^i$ and $\tilde{b}_j^o$ are $O(1/j^3)$, while the coefficients $\tilde{b}_j^i$ and $\tilde{a}_j^o$ are exponentially small, as $j \to \infty$.

6. Dirichlet problem in a half space

We now consider two classes of problems that can be expressed conveniently in terms of rectangular coordinates. In this section, we consider the problem of finding $u(x, y)$ satisfying

$$\nabla^2 u = 0, \quad -\infty < x < \infty, \quad y > 0, \tag{39}$$

with

$$u = g(x), \quad \text{on } y = 0, \quad \text{and} \quad u \to \text{constant, as } y \to \infty, \tag{40}$$

where $g(x) = g(x + 2\pi)$ is specified. Separation of variables leads to the representation

$$u(x, y) = \lim_{N\to\infty} u_N(x, y),$$

$$u_N(x, y) = \frac{a_0}{2} + \sum_{j=1}^{N} \mathrm{e}^{-jy}(a_j \cos(jx) + b_j \sin(jx)), \quad N = 1, 2, \ldots, \tag{41}$$

where $\{a_j, b_j\}$ are the Fourier coefficients of g defined in (1).

Following the same ideas as in Sections 3 and 4, in order to find a 'better' sequence of approximations to u, we first construct the harmonic extensions $\varphi_n(x, y)$ of $S_n(x)$ into the upper half plane. Using the same reasoning as in Section 3, we find

$$\begin{aligned}\varphi_n(x, y) &= \frac{a_{n,0}}{2} + \sum_{j=1}^{\infty} \mathrm{e}^{-jy}\{a_{n,j} \cos(jx) + b_{n,j} \sin(jx)\} \\ &= \mathrm{Re}\left\{\frac{a_{n,0}}{2} + \sum_{j=1}^{\infty}(a_{n,j} + ib_{n,j})w^j\right\}, \quad w = \mathrm{e}^{-y-ix}.\end{aligned} \tag{42}$$

Thus, the closed-form expressions for $\varphi_n(x, y)$ are given by the corresponding expressions in (14)–(15) with r replaced by e^{-y} and θ replaced by x. In particular,

$$\varphi_0(x, y) = \frac{1}{2\pi}\{2 \cosh(y/2) \cos(x/2) \cdot AT - \sinh(y/2) \sin(x/2) \cdot L\}, \tag{43}$$

$$\varphi_1(x, y) = \frac{1}{\pi}\{\sinh(y/2) \cos(x/2) \cdot L + 2 \cosh(y/2) \sin(x/2) \cdot AT\}, \tag{44}$$

where now

$$AT \equiv \tan^{-1}\left(\frac{\sin(x/2)}{\sinh(y/2)}\right), \qquad L \equiv \log\left(\frac{\cosh(y/2) + \cos(x/2)}{\cosh(y/2) - \cos(x/2)}\right).$$

To construct a more rapidly converging sequence of approximations to u, for any nonnegative integer M we first define $\tilde{S}_M(x)$ in terms of the singularities of g, as in Section 2, and then define

$$\tilde{\varphi}_M(x, y) \equiv \sum_{k=0}^{M} \sum_{s=1}^{n} A_{k,s} \varphi_k(x - x_s, y). \tag{45}$$

Here the constants $\{A_{k,s}\}$ are defined in (7) in terms of the singularities of g, and the harmonic functions $\{\varphi_k\}$ are defined by (42).

We now look for a solution for u in the form

$$u(x, y) = \tilde{\varphi}_M(x, y) + v(x, y), \tag{46}$$

where v satisfies

$$\nabla^2 v = 0, \quad -\infty < x < \infty, \quad y > 0,$$

with

$$v = g(x) - \tilde{S}_M(x), \quad \text{on } y = 0, \quad \text{and } v \to \text{constant, as } y \to \infty.$$

Since the boundary data for v is at least $C^M[-\pi, \pi]$, the approximate solutions for v obtained by separation of variables, analogous to (41), will converge faster than the corresponding approximate solutions $\{u_N\}$ for u. Thus, for any positive integer N, we define new approximations $u^{(M,N)}$ for u as

$$u^{(M,N)}(x, y) = \tilde{\varphi}_M(x, y) + v^{(M,N)}(x, y), \tag{47}$$

with

$$v^{(M,N)}(x, y) = \frac{\tilde{a}_0^{(M)}}{2} + \sum_{j=1}^{N} \mathrm{e}^{-jy} (\tilde{a}_j^{(M)} \cos(jx) + \tilde{b}_j^{(M)} \sin(jx)), \tag{48}$$

where $v^{(M,N)}$ is a partial-sum approximation to v, and the coefficients $\{\tilde{a}_j^{(M)}, \tilde{b}_j^{(M)}\}$, which are defined in (9)–(10), are just the Fourier coefficients of $g(x) - \tilde{S}_M(x)$.

To illustrate these results, we let

$$g(x) = \begin{cases} \frac{1}{2}\pi, & -\pi < x < -\frac{1}{2}\pi, \\ x, & -\frac{1}{2}\pi < x < \frac{1}{2}\pi, \\ -\frac{1}{2}\pi, & \frac{1}{2}\pi < x < \pi, \end{cases}$$

from which we find $a_j = 0$, $j \geqslant 0$, and $b_j = (-1)^j/j - (2/j)\cos(j\pi/2) + (2/\pi j^2)\sin(j\pi/2)$, $j \geqslant 1$. The approximation $u_{11}(x, y)$, defined in (41) with $N = 11$, is plotted in Figure 9. The oscillations in u_{11} near the boundary $y = 0$ due to the discontinuities in g are obvious.

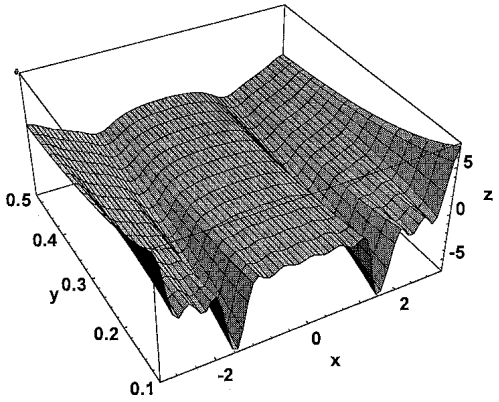

Figure 11. The approximation $\partial u_{11}/\partial x$ to $\partial u/\partial x$, obtained by differentiating (41) with $N = 11$, for the example of Section 6.

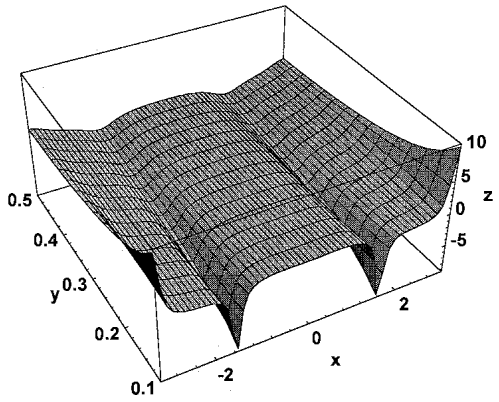

Figure 12. The approximation $\partial u^{(0,3)}/\partial x$ to $\partial u/\partial x$, obtained by differentiating $u^{(0,3)}(x, y)$ from (47)–(48) with $M = 0$ and $N = 3$, for the example of Section 6.

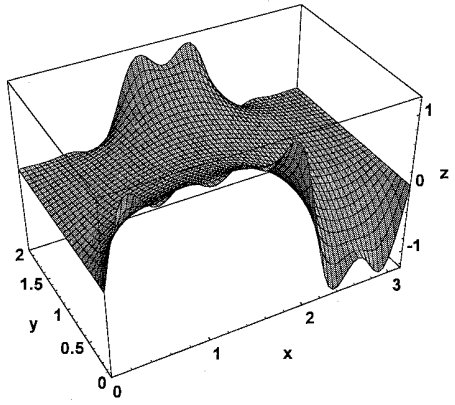

Figure 13. The approximation $u_{11}(x, y)$ from (52) with $N = 11$ for the example of Section 7, with $g_L(y) = 0 = g_R(y)$, and $g_B(x)$ and $g_T(x)$ given by (65)–(66).

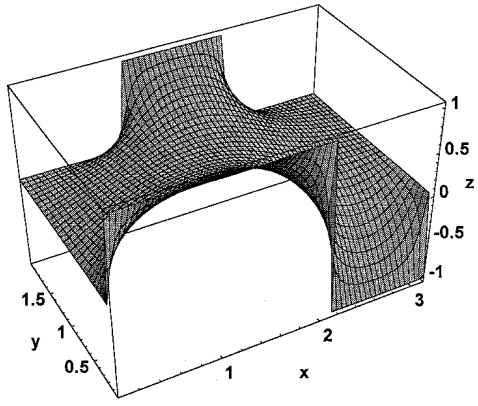

Figure 14. The approximation $u^{(0,3)}(x, y)$ from (63)–(64) with $M = 0$ and $N = 3$ for the example of Section 7, with $g_L(y) = 0 = g_R(y)$, and $g_B(x)$ and $g_T(x)$ given by (65)–(66).

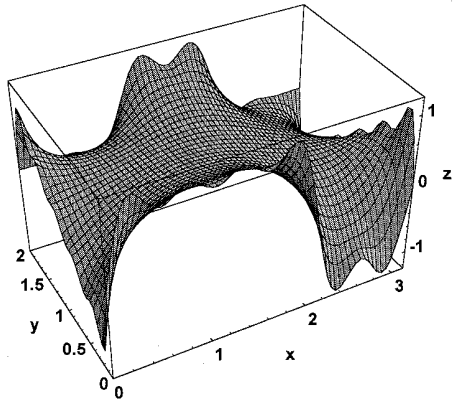

Figure 15. The approximation $u_{11}(x, y)$ from (52) with $N = 11$ for the example of Section 7, with $g_L(y) = y - 1 = -g_R(y)$, and $g_B(x)$ and $g_T(x)$ given by (65)–(66).

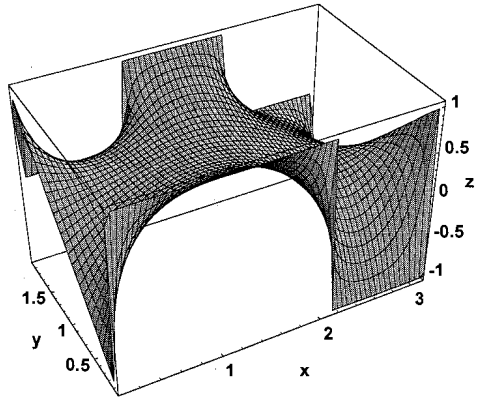

Figure 16. The approximation $u^{(0,3)}(x, y)$ from (63)–(64) with $M = 0$ and $N = 3$ for the example of Section 7, with $g_L(y) = y - 1 = -g_R(y)$, and $g_B(x)$ and $g_T(x)$ given by (65)–(66).

To construct a better approximation to u, we first note that g has three singularities in the interval $(-\pi, \pi]$, and hence we set $n = 3$, with $x_1 = -\pi/2$, $x_2 = \pi/2$, and $x_3 = \pi$. From the definition of g and (7), we find $A_{0,1} = -\pi$, $A_{0,2} = -\pi$, $A_{0,3} = \pi$, $A_{1,1} = 1$, $A_{1,2} = -1$, and $A_{1,3} = 0$. Using these values, we can compute $\tilde{\varphi}_0(x, y)$ from (45) with $M = 0$, and then $u^{(0,N)}(x, y)$ can be computed from Equations (47)–(48) with $M = 0$. In a similar manner, we construct $u^{(1,N)}$ by first computing $\tilde{\varphi}_1(x, y)$ from (45) with $M = 1$, and then computing $u^{(1,N)}(x, y)$ from (47)–(48) with $M = 1$. The approximation $u^{(0,3)}$, which is plotted in Figure 10, is a definite improvement over the approximation u_{11}, even though considerably fewer terms in the Fourier-series part of the approximation have been used. For this example we find

$$\|u - u_{11}\|_\infty \cong 1{\cdot}57, \qquad \|u - u^{(0,3)}\|_\infty \cong 0{\cdot}08, \quad \text{and} \quad \|u - u^{(1,3)}\|_\infty \cong 0{\cdot}008.$$

In some applications, it might be of interest to find approximations to various derivatives of u, as well as to u itself. To illustrate this possibility, the approximations $\partial u_{11}/\partial x$ and $\partial u^{(0,3)}/\partial x$ to $\partial u/\partial x$ are plotted in Figures 11 and 12, respectively. In this case, the approximation $\partial u_{11}/\partial x$ is 'meaningless' near $y = 0$, since the approximations $\{\partial u_N/\partial x\}$ do not converge at $y = 0$. The approximation $\partial u^{(0,3)}/\partial x$ is a definite improvement over $\partial u_{11}/\partial x$, while $\partial u^{(1,3)}/\partial x$ is an even better approximation to $\partial u/\partial x$. For this example, we find

$$\left\| \frac{\partial u}{\partial x} - \frac{\partial u_{11}}{\partial x} \right\|_\infty \cong 12{\cdot}52, \qquad \left\| \frac{\partial u}{\partial x} - \frac{\partial u^{(0,3)}}{\partial x} \right\|_\infty \cong 0{\cdot}50,$$

$$\left\| \frac{\partial u}{\partial x} - \frac{\partial u^{(1,3)}}{\partial x} \right\|_\infty \cong 0{\cdot}06.$$

7. Dirichlet problem in a rectangle

We now consider the problem of finding the function $u(x, y)$ which is harmonic inside a (finite) rectangular region of the x, y-plane, with u specified on the boundary of the rectangle. Thus, after an appropriate rescaling (if necessary), u satisfies the conditions

$$\nabla^2 u = 0, \quad 0 < x < \pi, \quad 0 < y < c, \tag{49}$$

with

$$\begin{aligned} &u(x, 0) = g_B(x), \qquad u(x, c) = g_T(x), \quad 0 < x < \pi, \\ &u(0, y) = g_L(y), \qquad u(\pi, y) = g_R(y), \quad 0 < y < c. \end{aligned} \tag{50}$$

Here, the functions g_B, g_T, g_L, and g_R, as well as the constant c, where $0 < c < \infty$, are specified. By superposition, we can write $u = u^{(1)} + u^{(2)}$, where $u^{(1)}$ satisfies conditions (49)–(50) with $g_L = g_R = 0$, and $u^{(2)}$ satisfies conditions (49)–(50) with $g_B = g_T = 0$. Thus, by a straightforward change of variables, it is sufficient to consider the problem (49)–(50) in detail only for the case when

$$g_L(y) = g_R(y) = 0. \tag{51}$$

To begin, we extend the definitions of g_B and g_T in an *odd, 2π-periodic manner* and then use separation of variables to find the approximate solutions

$$u_N(x, y) = \sum_{j=1}^{N} \{b_j^T \sinh(jy) + b_j^B \sinh(j(c-y))\} \frac{\sin(jx)}{\sinh(jc)}, \tag{52}$$

where $\{b_j^B\}$ and $\{b_j^T\}$ are the Fourier coefficients of (the odd, 2π-periodic extensions of) g_B and g_T, respectively.

To construct a more rapidly converging sequence of approximations to u, we first find the harmonic extension of $S_n(x - x_0)$, say, $\hat{\varphi}_n(x, y; x_0)$, for $0 < x < \pi$, $y > 0$, which *also* satisfies the conditions that it vanishes for $x = 0$ and $x = \pi$. Here, x_0 satisfies $0 \leqslant x_0 \leqslant \pi$ and represents a point where the boundary data $g_B(x)$ and/or $g_T(x)$ has a singularity. For $0 < x_0 < \pi$, using the function φ_n defined in (42), we can easily verify that

$$\begin{aligned} \hat{\varphi}_n(x, y; x_0) &\equiv \varphi_n(x - x_0, y) + (-1)^n \varphi_n(x + x_0, y) \\ &= \sum_{j=1}^{\infty} \hat{b}_{n,j}(x_0)\, \mathrm{e}^{-jy} \sin(jx), \quad \text{for } 0 < x_0 < \pi, \end{aligned} \tag{53}$$

where

$$\hat{b}_{n,j}(x_0) \equiv \begin{cases} 2\cos(jx_0) b_{n,j}, & n \text{ even}, \\ 2\sin(jx_0) a_{n,j}, & n \text{ odd}, \end{cases} \qquad \text{for } 0 < x_0 < \pi, \tag{54}$$

satisfies the conditions we require of $\hat{\varphi}_n$. For $x_0 = 0$ or $x_0 = \pi$, we first note that, since the boundary data has been extended in an *odd* fashion, $[g^{(2k+1)}(0)] = 0 = [g^{(2k+1)}(\pi)]$, where g denotes either g_B or g_T. Thus, for these values of x_0, we only need to define $\hat{\varphi}_n$ for n even, which we do by the formulas

$$\hat{\varphi}_n(x, y; x_0) \equiv \varphi_n(x - x_0, y) = \sum_{j=1}^{\infty} \hat{b}_{n,j}(x_0)\, \mathrm{e}^{-jy} \sin(jx), \quad x_0 = 0, \pi, \tag{55}$$

$$\hat{b}_{n,j}(x_0) \equiv \cos(jx_0) b_{n,j}, \quad \text{for } x_0 = 0, \pi, \quad n \text{ even}. \tag{56}$$

Following the ideas of Section 5, we define the harmonic functions

$$\tilde{\varphi}_M^B(x, y) \equiv \sum_{k=0}^{M} \sum_{s=1}^{n_B} A_{k,s}^B \hat{\varphi}_k(x, y; x_{B,s}), \tag{57}$$

and

$$\tilde{\varphi}_M^T(x, y) \equiv \sum_{k=0}^{M} \sum_{s=1}^{n_T} A_{k,s}^T \hat{\varphi}_k(x, c - y; x_{T,s}). \tag{58}$$

In (57)–(58), the constants $\{A_{k,s}^B\}$ and $\{A_{k,s}^T\}$ are defined by (7) in terms of the singularities of g_B and g_T, respectively. Here, $\{x_{B,s}\}$, $s = 1, 2, \ldots, n_B$, and $\{x_{T,s}\}$, $s = 1, 2, \ldots, n_T$,

denote the *locations* of the singularities of (the odd, 2π-periodic extensions of) g_B and g_T, respectively, which lie in the interval $0 \leqslant x \leqslant \pi$, while the functions $\{\hat{\varphi}_k\}$ are defined in (53)–(56). We then write u as

$$u(x, y) = \tilde{\varphi}_M^B(x, y) + \tilde{\varphi}_M^T(x, y) + v(x, y), \tag{59}$$

where v satisfies

$$\nabla^2 v = 0, \quad 0 < x < \pi, \quad 0 < y < c, \tag{60}$$

with

$$v = 0, \quad \text{on } x = 0 \quad \text{and} \quad x = \pi, \quad 0 < y < c,$$

$$v = \{g_B(x) - \tilde{\varphi}_M^B(x, 0)\} - \tilde{\varphi}_M^T(x, 0), \quad \text{on } y = 0, \quad 0 < x < \pi, \tag{61}$$

and

$$v = \{g_T(x) - \tilde{\varphi}_M^T(x, c)\} - \tilde{\varphi}_M^B(x, c), \quad \text{on } y = c, \quad 0 < x < \pi. \tag{62}$$

Again we note that, in the boundary conditions (61)–(62), the term in brackets on the right side of each equation is $C^M[-\pi, \pi]$, at least, while the last term is analytic for $0 \leqslant x \leqslant \pi$. Thus, the solution for v obtained by separation of variables will converge much faster than the corresponding solution for u.

We now solve the problem (60)–(62) for v by separation of variables, and then use (59) to define the new approximations $u^{(M,N)}$ for u as

$$u^{(M,N)}(x, y) = \tilde{\varphi}_M^B(x, y) + \tilde{\varphi}_M^T(x, y) + v^{(M,N)}(x, y), \tag{63}$$

where

$$v^{(M,N)}(x, y) \equiv \sum_{j=1}^{N} \{\tilde{b}_j^T \sinh(jy) + \tilde{b}_j^B \sinh(j(c - y))\} \frac{\sin(jx)}{\sinh(jc)},$$

$$\tilde{b}_j^B = b_j^B - \sum_{k=0}^{M} \sum_{s=1}^{n_B} A_{k,s}^B \hat{b}_{k,j}(x_{B,s}) - \mathrm{e}^{-jc} \sum_{k=0}^{M} \sum_{s=1}^{n_T} A_{k,s}^T \hat{b}_{k,j}(x_{T,s}), \tag{64}$$

$$\tilde{b}_j^T = b_j^T - \sum_{k=0}^{M} \sum_{s=1}^{n_T} A_{k,s}^T \hat{b}_{k,j}(x_{T,s}) - \mathrm{e}^{-jc} \sum_{k=0}^{M} \sum_{s=1}^{n_B} A_{k,s}^B \hat{b}_{k,j}(x_{B,s}),$$

for $j = 1, 2, \ldots, N$. Here the coefficients $\{\hat{b}_{n,j}(x_0)\}$ are defined in (54) and (56).

To illustrate these results, we set $c = 2$ and let

$$g_B(x) = \begin{cases} 1, & 0 < x < 2\pi/3, \\ -1, & 2\pi/3 < x < \pi, \end{cases} \tag{65}$$

and

$$g_T(x) = \begin{cases} 0, & 0 < x < \pi/3, \\ 1, & \pi/3 < x < 2\pi/3, \\ 0, & 2\pi/3 < x < \pi, \end{cases} \tag{66}$$

from which we find

$$b_j^B = \frac{2}{j\pi}(1 + (-1)^j - 2\cos(2j\pi/3)), \qquad b_j^T = \frac{2}{j\pi}(\cos(j\pi/3) - \cos(2j\pi/3)),$$

for $j \geqslant 1$. The approximation $u_{11}(x, y)$ which we obtained by inserting these coefficients into Equation (52) with $N = 11$ is plotted in Figure 13. The (unwanted) oscillations in u_{11}, particularly near the boundary, due to the discontinuities in g_B and g_T, are apparent.

To construct a better approximation to u, we first note that (the odd, 2π-periodic extension of) g_B has three singularities in the interval $[0, \pi]$, while g_T has two singularities in this interval. Hence, we set $n_B = 3$ and $n_T = 2$, with $x_{B,1} = 0$, $x_{B,2} = 2\pi/3$, $x_{B,3} = \pi$, $x_{T,1} = \pi/3$, and $x_{T,2} = 2\pi/3$. From the definitions of g_B and g_T, and using (7), we find $A_{0,1}^B = 2$, $A_{0,2}^B = -2$, $A_{0,3}^B = 2$, $A_{0,1}^T = 1$, and $A_{0,2}^T = -1$. Using these values in (57)–(58), we find

$$\tilde{\varphi}_0^B(x, y) = 2\{\hat{\varphi}_0(x, y; 0) - \hat{\varphi}_0(x, y; 2\pi/3) + \hat{\varphi}_0(x, y; \pi)\},$$

$$\tilde{\varphi}_0^T(x, y) = \hat{\varphi}_0(x, c - y; \pi/3) - \hat{\varphi}_0(x, c - y; 2\pi/3),$$

where $\hat{\varphi}_0(x, y; x_0)$ is defined in (53)–(56) with $n = 0$. We then use these expressions, along with the definitions in (63)–(64), to construct the approximation $u^{(0,3)}(x, y)$, which is plotted in Figure 14. The higher quality of the approximation $u^{(0,3)}$, compared to u_{11} (especially near the boundary), is obvious, and, in fact, we find

$$\|u - u_{11}\|_\infty \cong 1{\cdot}0 \quad \text{and} \quad \|u - u^{(0,3)}\|_\infty \cong 9{\cdot}0 \times 10^{-3}. \tag{67}$$

The solution for the case when g_L and g_R are specified, and with $g_B = g_T = 0$, can be obtained from the solution we have just constructed by using the transformations

$$x \to \frac{\pi y}{c}, \qquad y \to \frac{\pi x}{c}, \qquad c \to \frac{\pi^2}{c}, \qquad b_j^B \to b_j^L, \qquad b_j^T \to b_j^R.$$

This solution can then be combined with the solution constructed above to obtain the general solution when all of the functions g_B, g_T, g_L, and g_R are specified, as described at the beginning of this section. To illustrate this technique, we let g_B and g_T be defined by Equations (65)–(66), and also let

$$g_L(y) = y - 1 = -g_R(y).$$

In Figure 15, the approximation $u_{11}(x, y)$ is plotted, while the approximation $u^{(0,3)}(x, y)$ is plotted in Figure 16. In this case, the maximum norm errors are again given by (67).

8. Discussion

The method presented here appears to provide a practical way to obtain 'very accurate' approximations to the solutions, u, of at least two classes of Dirichlet problems for Laplace's equations with discontinuous boundary data. The method is constructive, and only requires a knowledge of the locations and magnitudes of the discontinuities in the data. In *theory*, the method can be used to construct a *sequence of approximations which converges exponentially to the solution in the maximum norm*. (This follows from the observation that the maximum absolute value of the harmonic function $u - u^{(M,N)}$ occurs on the boundary of the domain of interest, and, on the boundary, $u - u^{(M,N)} = \tilde{g} \equiv g - \tilde{S}_M - g^{(M,N)}$, where $g^{(M,N)}$ denotes the first $2N+1$ terms in the Fourier-series representation of $g - \tilde{S}_M$. From the main result of [8], it follows that, if we set $N = \lambda M$, where λ is an appropriate positive constant, then $\tilde{g}$ approaches zero exponentially as $M \to \infty$. Hence, $u - u^{(M,\lambda M)}$ also approaches zero exponentially as $M \to \infty$. See [8] for more details.) In particular, this implies that the (unwanted) effects of Gibbs phenomenon *can be completely overcome*! In *practice*, the method can be viewed as one that can provide a 'very accurate' approximation, $u^{(M,N)}$, to u, and $u^{(M,N)}$ contains relatively *few terms*. This is the aspect of the method that is illustrated by the examples in the previous sections.

A special case of the type of problems considered here has been studied by Shi and Hassard [12]. They consider the case when the domain of interest is the unit square and the boundary data is expressed in terms of continuous, 'elementary' functions. Their technique appears to involve several more 'steps' than the method presented here, and is designed to handle discontinuities only at the corners of the square. As demonstrated above, the present method can handle discontinuities along the edges of a square, as well as discontinuities at the corners.

Applications of some of the ideas discussed to the solution of Laplace's equation in more general two-dimensional domains (such as multiply connected domains) may also be possible. For example, Bird and Steele [13] present a solution procedure for the two-dimensional Laplace's equation on circular domains with circular holes, and with arbitrary boundary conditions. The 'interaction' of the different boundaries is expressed simply and accurately, which results in an efficient solution algorithm. They assume, in essence, that the boundary data can be represented as a uniformly convergent Fourier series, and the only simplification they make is that the boundary data can be 'accurately' represented by only a finite number of terms in the appropriate Fourier series. This assumption will not be valid, of course, if some of the data is discontinuous. However, for such multiply connected domains, it should be rather straightforward to combine their ideas with those presented here to construct a solution algorithm valid for discontinuous boundary data.

Although attention here has been restricted to Laplace's equation, the basic method will undoubtedly find application to more general elliptic problems, as well as to other classes of partial differential equations. For example, the method as described here may be directly applicable, along with the superposition principle, to boundary value problems which involve equations which contain the Laplacian operator and another linear operator. To see this, suppose we wish to find w satisfying

$$\nabla^2 w + \mathfrak{L}(w) = f, \quad \text{in } \mathfrak{D}, \quad \text{with } w = g, \quad \text{on } \partial\,\mathfrak{D},$$

where $\partial\mathfrak{D}$ denotes the boundary of the (two-dimensional) domain $\mathfrak{D}$. Here $\mathfrak{L}$ is a linear operator, $\mathfrak{D}$ has either circular or rectangular boundaries (as discussed above), and g has one or more points of discontinuity on $\partial\mathfrak{D}$. We then set $w = u + v$, where u satisfies

$$\nabla^2 u = 0, \quad \text{in } \mathfrak{D}, \qquad \text{with} \quad u = g, \quad \text{on } \partial\,\mathfrak{D}.$$

Then v satisfies

$$\nabla^2 v + \mathfrak{L}(v) = \tilde{f} \equiv f - \mathfrak{L}(u), \quad \text{in } \mathfrak{D}, \quad \text{with } v = 0, \quad \text{on } \partial\mathfrak{D}.$$

The solution for u can be accurately approximated, as described above, while the problem for v involves homogeneous boundary data (although $\tilde{f}$ has some discontinuities on $\partial\,\mathfrak{D}$). In particular, if $\mathfrak{L}$ involves only derivatives with respect to a variable, or variables, other than x and y (or r and θ), then $\mathfrak{L}(u) \equiv 0$ and the problem for v is identical to the problem for u, except that the boundary data is identically zero. This will be the case, for example, if $\mathfrak{L}(w) = -w_t$, or $\mathfrak{L}(w) = -w_{tt}$, as in the heat or wave equation, and if g is independent of t.

In addition, the method may be useful when applied in conjunction with a variety of purely numerical methods, such as spectral methods, boundary-element methods, or finite-element methods. For such applications, it is convenient to think of the method as providing a smooth (analytic) extension of discontinuous boundary data into the interior of the domain of interest. It might then be possible to write the desired solution, u, as a sum of appropriate multiples of the functions $\varphi_n(r, \theta)$ or $\varphi_n(x, y)$, as defined in Sections 3 and 6, respectively, and a new (unknown) function v, which would satisfy much smoother boundary conditions. Only the function v would need to be approximated by the numerical method being used.

References

1. D. Gottlieb, C. Shu, A. Solomonoff and H. Vandeven, On the Gibbs phenomena I: recovering exponential accuracy from the Fourier partial sum of a non-periodic analytic function. *J. Comp. Appl. Math.* 43 (1992) 81–98.
2. D. Gottlieb and C. Shu, Resolution properties of the Fourier method for discontinuous waves. *Comp. Meth. Appl. Mech. Eng.* 116 (1994) 27–37.
3. D. Gottlieb and C. Shu, On the Gibbs phenomena III: recovering exponential accuracy in a sub-interval from a spectral partial sum of a piecewise analytic function. *SIAM J. Num. Anal.* 33 (1996) 280–290.
4. D. Gottlieb and C. Shu, On the Gibbs phenomena IV: Recovering exponential accuracy in a sub-interval from a Gegenbauer partial sum of a piecewise analytic function. *Math. Comp.* 64 (1995) 1081–1096.
5. D. Gottlieb and C. Shu, On the Gibbs phenomena V: Recovering exponential accuracy from collocation point values of a piecewise analytic function. *Num. Math.* (to appear).
6. J. F. Geer, Rational trigonometric approximations using Fourier series partial sums. *J. Sci. Comp.* 10 (1995) 325–356.
7. J. N. Lyness, Computational techniques based on the Lanczos representation. *Math. Comp.* 28 (1974) 81–123.
8. J. F. Geer and N. S. Banerjee, Exponentially accurate approximations to piece-wise smooth periodic functions. *J. Sci. Comp.* 12 (1997) 253–287.
9. N. S. Banerjee and J. F. Geer, Exponentially accurate approximations to periodic Lipschitz functions based on Fourier series partial sums. *SIAM J. Sci. Comp.* (to appear).
10. N. K. Bary, *A Treatise on Trigonometric Series, Vol. 1*. New York: MacMillan (1964) 553pp.
11. S. Wolfram, *Mathematica: A System for Doing Mathematics by Computer* (Second edition). New York: Addison Wesley (1991) 961pp.
12. Z. Shi and B. Hassard, Precise solution of Laplace's equation. *Math. Comp.* 64 (1995) 515–536.
13. M. D. Bird and C. R. Steele, A solution procedure for Laplace's equation on multiply connected circular domains. *J. Appl. Mech.* 114 (1992) 398–404.